

Synthesis, Characterization, Antimicrobial activity and Anti-cancerous efficacy (HeLa cell lines) by *Gracilaria corticata* mediated synthesized silver nanoparticles

¹Subramanian Poornima, ^{1*}Karupppiah Valivittan

Department of Biotechnology, St. Peter's University, Avadi, Chennai-600054

Abstract:

This work presents a simple method for the green synthesis of silver nanoparticles (AgNPs) using from red algae *Gracilaria corticata* present in the coast of Rameshwaram near mandapam camp. The AgNPs were prepared using silver nitrate solution and aqueous extract of algae at stirring for 30 min at 90°C. The formation of silver nanoparticles was monitored by measurements of UV-vis and FT-IR and characterized by size and zeta potential measurements using DLS and morphologically by TEM. The UV-vis absorption spectrum showed the surface plasmon peak at 385 nm, which is characteristic peak of silver nanoparticles. The functional biomolecules present in the polysaccharide and the interaction between the nanoparticles were identified by the Fourier transform infrared spectroscopy (FT-IR) analysis. XRD results shown that it is a Face Centered Cubic Lattice Structure (111), the hydrodynamic diameter of the AgNPs varied between 84.8nm and Zeta potential of the silver nanoparticles was 12.5mV. The AgNPs were tested for antimicrobial activity using (Gram-Positive and negative bacteria, fungal species) and Anti-cancer studies was done by using HeLa cell lines at in-vitro studies

Keywords - *Gracilaria corticata*, Silver nanoparticles, Anti-cancer activity, Antimicrobial activity.

Introduction

The increased emergence of drug-resistant microbes is a major challenge for the scientific community in the continuous successful development of effective therapeutics. Silver nanoparticles (AgNPs) are known for their antimicrobial properties, being effective against pathogens, which explain their potential for several biotechnological applications, in addition to their electrical, thermal, magnetic, and catalytic characteristics (Mohanty et al., 2012; Mubarak Ali et al., 2011). However, AgNPs show high reactivity, requiring adequate stabilization during and after the process of synthesis to prevent oxidation and aggregation of particles over time. Since the development of the concept of green nanoparticle preparation, there has been growing demand for environment-friendly processes of metal-nanoparticle synthesis that does not employ toxic chemicals (Thovhogi et al., 2015).

Although several conventional methods of producing pure and well-defined nanoparticles exist, most of these methods are expensive and employ physical processes or chemical reduction with strong reducing agents. In addition, many stabilizers used in these processes, particularly surfactants, may themselves present significant cellular toxicity, which can severely limit the use (Thakkar et al., 2010). Nanoparticles based noble metals have been produced by green synthesis, using compounds such as ZnO, CdO and Sm₂O₃, among others, without the use of toxic reagents and with the smallest sizes (Diallo et al., 2015; Thema et al., 2015a,b; Thovhogi et al., 2015; Sone et al., 2015).

Among the substances used in various methods of synthesis, such as extract and gum, the polysaccharides have been shown to be excellent candidates for stabilizing and controlling the size of nanoparticles (NPs). The stabilization provided by polysaccharides relies on the presence of multiple binding sites along the polysaccharide chain to facilitate attachment to the metal's surface, thereby effectively "trapping" the metal nanoparticle and conferring significant protection against aggregation and chemical modification. Stable silver nanoparticles have been synthesized by the use of polysaccharides, such as starch (Konwarh et al., 2011), Chitosan (Tran et al., 2010), natural gums (Quelemes et al., 2013), marine polysaccharides (Venkatpurwar and Pokharkar, 2011), and hyaluronan (Xia et al., 2011). In all cases, the polymer plays a dual role as a stabilizer and a reducing agent.

This kind of approach allows the use of natural, inexpensive, and biocompatible materials as reducing agents in the synthesis of AgNPs; these agents are capable of providing sufficient stability in therapeutic applications even in the presence of electrolytes and under conditions of pH variation (Wijesekara et al., 2011). Red marine seaweeds are abundant along the Northeastern Brazilian coast and have high biological potential for providing compounds that have utility in industry, and an example is the *Gracilaria* genus that is common and represents an economic source for the region (Carneiro et al., 2014; Coura et al., 2012). Polysaccharides from the *Gracilaria* genus are composed mainly of the alternating 3-linked-β-D-galactopyranose unit and the 4-linked-3,6-anhydro-α-L-galactopyranose unit (Maciel et al.,

2008), where the L moiety may be substituted by methyl or sulfate groups. The polysaccharide isolated from marine algae has interesting functional properties, such as antioxidant (Souza et al., 2012), anticoagulant, and antiviral activities (Chattopadhyay et al., 2008).

In the present study, silver nanoparticles were prepared using a *Gracilaria corticata* isolated from red marine algae, which acted as both the reducing and stabilizing agents. This approach not only utilizes an abundant regional resource, but also falls within the scope of green synthesis for AgNPs that could allow scalability of the process to industrially relevant applications. In addition, we evaluated the antimicrobial activity (Bacteria and Fungi) and anticancer efficacy (HeLa cell lines) of the synthesized AgNPs.

Methodology

Materials

Silver nitrate (>99% pure) was purchased from Sigma Aldrich, India. Potato dextrose broth, Potato dextrose agar, Nutrient broth, Nutrient agar plate, was supplied by Hi-media, India.

Sample collection and preparation (*Gracilaria corticata*)

The red algae (*Gracilaria corticata*) were collected from the rameshwaram sea coast area, Tamilnadu, India and were brought to the nanotechnology laboratory and washed with distilled water several times to remove the impurities. The clean algae were dried at room temperature in the shade for a week and powdered using a mortar and pestle.

Preparation of *Gracilaria corticata* (red algae) extract

Dried powdered *Gracilaria corticata* (5g) was mixed with 100ml distilled water then the solution was kept for continues heating at 80°C for 1hour at room temperature with frequent shaking. After that the extract were filtered by using Whatmann No1 filter paper. The extract was collected and stored at 4°C for further use.

Synthesis of silver nanoparticles from *Gracilaria corticata*

10 ml of the aqueous extract of *Gracilaria corticata* was added into 90ml of aqueous solution of 1mM Silver nitrate. The mixture was exposed to a range of controlled temperatures for 24h. Appearance of brown color in solution indicated the formation of AgNPs. The solution was then kept in dark for further analysis collected and stored at 4°C for further use.

Collection of microbes (Bacteria and fungi)

The microbes (Bacteria and fungi) samples were collected from Department of Biotechnology, Thiruvalluvar University, Vellore, Tamil Nadu, India. These samples were stored in an ice box and transported to the laboratory for microbiological characterization. Through serial dilution pour plate technique, fungal sp. was isolated using potato dextrose agar (PDA) medium, and Gram negative and Gram-positive bacteria were isolated from nutrient agar medium. Further, it is maintained in potato dextrose agar slants (fungi) and nutrient agar slants (bacteria) for onward analysis.

Antimicrobial activity

Antibacterial activity of *Gracilaria corticata* produced AgNPs

The antibacterial activity of AgNPs was evaluated against the following pathogenic strains *E. coli*, *Pseudomonas Fluorescence*, *Staphylococcus aureus*, *Sphingobacterium thalpophilum*, *Legionella pneumonia*, *Actinomyces israelii*, *Enterobacter cloacae*, *Helicobacter pylori*, *Acinetobacter* and *Bacillus subtilis*. These cultures were grown on appropriate medium at 37°C for overnight incubation and maintained at 4°C in a refrigerator. Disc diffusion method disc of 5Mm was made for nutrient agar medium and each disc was dipped at different concentration (170, 100, 50 ppm) efficiency of prepared AgNPs. The pure cultures of bacterial pathogens were sub-cultured on an appropriate medium. For comparison, plate of the same diameter with 5Mm penicillin-g (30mcg) was used. After incubation at 37°C for 24h the zones of bacterial inhibition were measured. The assays were performed triplicate.

Antifungal activity of *Gracilaria corticata* produced AgNPs

The antifungal activity of AgNPs was evaluated against the following pathogenic strains *Aspergillus niger*, *Aspergillus flavus*, *Schelorosium rolfsii*, *Rhizopus oligosporus*, *Aspergillus acidus*, *Athelia rolfsii*, *Aspergillus fumigates*, *Rhizopus oryzae*, *Trichoderma asperellum* and *Meyerozyma caribbica*. These cultures were grown on appropriate medium at 37°C for overnight incubation and maintained at 4°C in a refrigerator. Disc diffusion method disc of 5Mm was made on nutrient agar medium and each disc was dipped at different concentration (170, 100, 50ppm) efficiency of prepared AgNPs. The pure cultures of fungal pathogens were sub-cultured on an appropriate medium. Discs of 5 mm diameter were made on potato dextrose agar medium. Each strain was swabbed uniformly onto the individual plate. For

comparison, plate of the same diameter with 5Mm itraconazole (30 mcg) was used. After incubation at 37°C for 24h the zones of fungal inhibition were measured. The assays were performed triplicate.

Anti cancer activity of *Gracilaria corticata* produced AgNPs towards (HeLa) cell lines

Cell line

The human cervical cancer cell line (HeLa) was obtained from National Centre for Cell Science (NCCS), Pune and grown in Eagles Minimum Essential Medium containing 10% fetal bovine serum (FBS). The cells were maintained at 37°C, 5% CO₂, 95% air and 100% relative humidity. Maintenance cultures were passaged weekly, and the culture medium was changed twice a week.

Cell treatment procedure

The monolayer cells were detached with trypsin-ethylenediaminetetraacetic acid (EDTA) to make single cell suspension. Viable cells were counted by trypan blue exclusion using a hemocytometer and diluted with medium containing 5% FBS to give final density of 1x10⁵ cells/ml. One hundred microlitres per well of cell suspension were seeded into 96-well plates at plating density of 10,000 cells/well and incubated to allow for cell attachment at 37°C, 5% CO₂, 95% air and 100% relative humidity. After 24 h the cells were treated with serial concentrations of the test samples.

They were initially dispersed in phosphate buffered saline (PBS) and an aliquot of the sample solution was diluted to twice the desired final maximum test concentration with serum free medium. Additional four serial dilutions were made to provide a total of five sample concentrations. Aliquots of 100 µl of these different sample dilutions were added to the appropriate wells already containing 100 µl of medium, resulting in the required final sample concentrations. Following sample addition, the plates were incubated for an additional 48 h at 37°C, 5% CO₂, 95% air and 100% relative humidity. The medium containing without samples were served as control and triplicate was maintained for all concentrations.

MTT assay

3-[4,5-dimethylthiazol-2-yl]2,5-diphenyltetrazolium bromide (MTT) is a yellow water soluble tetrazolium salt. A mitochondrial enzyme in living cells, succinate-dehydrogenase, cleaves the tetrazolium ring, converting the MTT to an insoluble purple formazan. Therefore, the amount of formazan produced is directly proportional to the number of viable cells.

After 48 h of incubation, 15µl of MTT (5mg/ml) in phosphate buffered saline (PBS) was added to each well and incubated at 37°C for 4h. The medium with MTT was then flicked off and the formed formazan crystals were solubilized in 100µl of DMSO and then measured the absorbance at 570 nm using micro plate reader. The percentage cell growth was then calculated with respect to control as follows

$$\% \text{ Cell Growth} = [\text{A}] \text{ Test} / [\text{A}] \text{ control} \times 100$$

Characterization of Ag nanoparticles

UV – Visible spectrum for synthesized nanoparticles

The nanoparticles were monitored by UV–visible spectrum at various time intervals. The UV – Visible spectra of this solution was recorded in spectra 50 ANALYTIKJENA Spectrophotometer, from 250 to 400nm.

FT-IR Analysis for synthesized nanoparticles

The nanoparticles were harvested and characterized by FT-IR. The FT-IR spectrum was taken in the mid IR region of 400–4000 cm⁻¹. The spectrum was recorded using ATR (attenuated total reflectance) technique. The sample was directly placed in the KBr crystal and the spectrum was recorded in the transmittance m

X-ray Diffraction analysis for synthesized nanoparticles

The nanoparticles were harvested and characterized by XRD and TEM. The XRD pattern was recorded using computer controlled XRD-system, JEOL, and Model: JPX-8030 with CuK radiation (Ni filtered = 13418 Å⁰) at the range of 40kV, 20A. The ‘peak search’ and ‘search match’ program built in software (syn master 7935) was used to identify the peak table and ultimately for the identification of XRD peak.

Particle Size and Zeta potential analyzer for synthesized nanoparticles

The aqueous suspension of the synthesized nanoparticles was filtered through a 0.22 µm syringe driven filter unit and the size of the distributed nanoparticles were measured by using the principle of Dynamic Light Scattering (DLS) technique made in a Nanopartica (HORIBA, SZ-100) compact scattering spectrometer.

Transmission electron microscopy (TEM)

The surface morphology and size of the nanoparticles were studied by transmission electron microscopy (JEOL (JEM-1010)) with an accelerating voltage of 80 kV. A drop of aqueous AgNPs on the carbon-coated copper TEM grids was dried and kept under vacuum in desiccators before loading them onto a specimen holder. The particle size and surface morphology of nanoparticles were evaluated using ImageJ 1.45s software.

Results and discussion

In the present study, the red algal *Gracilaria corticata* (**Fig. 1**) used in the green synthesis of AgNPs forming complexes with the silver ions and thereby controlling the process of reduction is to stabilize and protect the particles from aggregation. Used a green protocol for the synthesis of silver nanoparticles with algal extract extracted from *Gracilaria corticata*. In the present study, the seaweed *G. corticata* was used because it is very commonly found in Rameshwaram a simple procedure to extract from the algae was used.

UV-Visible spectral analysis (*Gracilaria corticata*)

It is well-known that silver nanoparticles exhibit brown color, which arises due to excitation of surface Plasmon vibrations of the silver nanoparticles. After addition of 1mM silver nitrate solution to the aqueous extract, the colour of the composition has been changed to dark brown colour. The maximum absorbance peak is observed at 385 nm for *Gracilaria corticata* (**Fig. 2**). The overall observations suggest that the bio reduction of (silver ions) Ag^+ to Ag^0 was confirmed by UV-Visible spectroscopy.

Fourier Transform Infrared Spectrophotometry analysis (*Gracilaria corticata*)

FT-IR spectrum of the biosynthesized silver nanoparticles using *Gracilaria corticata*. The absorption peaks at 3358, 2928, 2096, 1741, 1637, 1460, 1383, 1165 and 1050 cm^{-1} . The peak at 3358 cm^{-1} reveals the presence of N-H stretching vibration, indicating the primary and secondary amines, 2928 cm^{-1} reveals the presence of C-H stretching vibration, indicating the presence of carboxylic/phenolic groups, 2096 cm^{-1} reveals the presence of C-H stretching vibration, indicating the presence of alkanes, 2104 cm^{-1} reveals the presence of $-C\equiv C-$ stretching vibration, indicating the presence of alkynes, 1773, 1637 cm^{-1} reveals indicating the presence of [N-H] C=O group that is characteristic of proteins shifted from after the synthesis of AgNPs, 1460 and 1383 cm^{-1} reveals the presence of amide II and amide III of aromatic rings either may be poly phenols associated with synthesized silver nanoparticles which is segregated by *Gracilaria corticata* extract, 1165 and 1050 cm^{-1} corresponding to C-X stretching vibration of fluoroalkanes (**Fig.3**).

X-Ray Diffraction analysis (*Gracilaria corticata*)

The sample of AgNPs could be also characterized by X-Ray Diffraction analysis of dry powder. The diffraction intensities were recorded from 10°-80° at 2 θ angles (**Fig.4**). Four different and important characteristic peaks were observed at the 2 θ of 38.6°, 45.8° and 49.8° that correspond to (111), (200) and (220) planes, respectively. All the peaks in XRD pattern can be readily indexed to a face centered cubic structure of silver as per available literature (JCPDS, File No. 4-0781). The XRD pattern of these peaks indicates the AgNPs is crystalline in nature and some of the unassigned peaks were observed it may be due to the fewer bio-molecules of stabilizing agents are enzymes or proteins in the *Gracilaria corticata* extract.

Dynamic light scattering analysis (*Gracilaria corticata*)

The particle size distribution spectra for the silver nanoparticles were recorded as diameter (nm) verses frequency (%/nm) spectra with diameter (nm) on x-axis and frequency (%/nm) on y-axis. The zeta potential spectra for the silver nanoparticles were recorded zeta potential verses intensity spectra with zeta potential (mV) on x-axis and intensity (a.u) on y-axis. Dynamic light scattering technique has been used to measure hydrodynamic diameter of the hydrosol (particle suspension). *Gracilaria corticata* AgNPs was found to be 84.8nm (**Fig. 5a**) the recorded value of zeta potential of the silver nanoparticles was 12.5mV (**Fig. 5b**) which resulted in the agglomerated state of the formed AgNPs.

Transmission Electron Microscopic analysis (*Gracilaria corticata*)

Silver nanoparticles synthesized from *Gracilaria corticata* used in this study are having the mean diameter of 0.2 μm -20nm as shown by TEM micrographs (**Fig. 6**). The formed AgNPs appears slightly aggregated due to the absence of strong surface protecting ligands and found to be spherical in shape. The particles were crystalline in nature as revealed by the XRD analysis.

Antimicrobial activity of *Gracilaria corticata* extracts mediated silver nanoparticles

It is well-known that silver nanoparticles exhibit brown color, arising due to excitation of surface Plasmon vibrations in the silver nanoparticles. Silver nanoparticles obtained from *Gracilaria corticata* shown have very strong inhibitory

action against fungal sp, Gram-positive and Gram-negative bacteria. These isolates were collected from nanotechnology laboratory, Acharya N G Ranga Agricultural University, Tirupathi. Three concentrations of NPs (170, 100, 50ppm) were prepared and were applied against an array of bacterial species viz., *Escherichia coli*, *Staphylococcus aureus*, *Pseudomonas fluorescens*, *Sphingobacterium thalpophilum*, *Legionella pneumonia*, *Actinomyces israelii*, *Enterobacter cloacae*, *Helicobacter pylori*, *Acinetobacter* and *Bacillus subtilis*, fungal species viz., *Aspergillus niger*, *Aspergillus flavus*, *Sclerotium rolfsii*, *Rhizopus oligosporus*, *Aspergillus acidus*, *Athelia rolfsii*, *Aspergillus fumigates*, *Rhizopus oryzae*, *Trichoderma asperellum* and *Meyerozyma caribbica*. The higher concentration (170ppm) of AgNPs showed significant antimicrobial effect compared with other concentrations (100, 50ppm and antibiotic discs).

Following the silver nanoparticles treatment, the cytoplasm membrane shrank and became separated from the cell wall. Cellular contents were then released from the cell wall, and the cell wall was degraded. These phenomena suggest possible antibacterial mechanisms by which silver ions inhibit bacterial growth, as well as cellular responses of both the gram-positive and gram-negative bacteria to the silver ion treatment. Although the mechanisms underlying the antibacterial actions of silver are still not fully understood, several previous reports (Pal et al. 2007) showed that the interaction between silver and the constituents of the bacterial membrane caused structural changes and damage to the membranes and intracellular metabolic activity which might be the cause or consequence of cell death, as demonstrated in this study.

The mechanism by which the nanoparticles are able to penetrate the bacteria is not understood completely, but studies suggest that when bacteria were treated with silver nanoparticles, changes took place in its membrane morphology that produced a significant increase in its permeability affecting proper transport through the plasma membrane (Auffan et al., 2009), leaving the bacterial cells incapable of properly regulating transport through the plasma membrane, resulting into cell death (Supraja et al., 2015). It is observed that silver nanoparticles have penetrated inside the bacteria and have caused damage by interacting with phosphorus- and sulfur-containing compounds such as DNA (He et al., 2008). Moreover, *Gracilaria corticata* and AgNPs showed good antibacterial and antifungal activity (**Fig. 7a and 7b**), (**Table. 1 and 2**). The findings in this study may lead to the development of AgNPs-based new antimicrobial systems for medical applications.

Anti cancer activity of HeLa (Human Cervical cancer cell lines)

The cytotoxic effect of *Gracilaria corticata* mediated synthesis of AgNPs was evaluated in vitro against Human cervical cancer cell lines (HeLa) cell lines at five different concentrations (12.5, 25, 50, 100 and 200µg/mL) by MTT assay and the results are depicted in (**Fig. 8 and 9**). The in vitro screening of the synthesized AgNPs exhibited the percentage viability of HeLa cell lines decreased with increased concentration of AgNPs in a dose dependent manner (Turner and Timothy, 2012). This study clearly indicated that the size and dose of AgNPs as well as cells used in the experiment play a crucial role in the cytotoxic effect of AgNPs. AgNPs exhibited low viable cells 71% at 200 µg/mL and high viable cells 97% at 12.5 µg/ml concentration in *Gracilaria corticata*. It showed potential distinct anticancer activity on the tested cell lines. Similarly, the cytotoxic effect exhibited by different types of silver nanoparticles on HeLa cell line and the variance due to concentration of nanoparticles (**Table. 3**).

The experimental results in the present study indicated that the silver nanoparticles has anticancer activity through induction of apoptosis in HeLa cancer cell line, suggesting that AgNPs might be a potential alternative therapeutic agent for human cancer. The morphological changes of HeLa cancer cells were observed in this study when they were treated with AgNPs with different concentrations. They suggested that generation of reactive oxygen species plays key role in the induction of apoptosis in HeLa cancer cells.

Conclusion

In the present study, we demonstrated the stable green synthesis of an AgNP solution with red algae *Gracilaria corticata* reducing and stabilizing agent. The resulted particles exhibited favorable characteristics, including the spherical shape, hydrodynamic diameter between 84.8 nm and positive zeta potential 12.5mv. The synthesized AgNPs showed very good antimicrobial activity with greater efficacy against bacteria than fungi, probably due to the shape and the size of AgNP, Anti-cancer efficacy of HeLa cell lines showed very less cytotoxicity. This kind of study may also serve as a model for the future preparation of nano-medicines, Agricultural spraying and Industrial Applications.

References

- [1] Mohanty, S., Mishra, S., Jena, P., Jacob, B., Sarkar, B., Sonawane, A., 2012. An investigation on the antibacterial, cytotoxic, and antibiofilm efficacy of starch-stabilized silver nanoparticles. *Nanomed. Nanotechnol. Biol. Med.* 8, 916–924. <http://dx.doi.org/10.1016/j.nano.2011.11.007>.
- [2] MubarakAli, D., Thajuddin, N., Jeganathan, K., Gunasekaran, M., 2011. Plant extract mediated synthesis of silver and gold nanoparticles and its antibacterial activity against clinically isolated pathogens. *Colloids Surf. B Biointerfaces* 85, 360–365. <http://dx.doi.org/10.1016/j.colsurfb.2011.03.009>.

- [3] Thovhogi, N., Diallo, A., Gurib-Fakim, A., Maaza, M., 2015. Nanoparticles green synthesis by Hibiscus Sabdariffa flower extract: main physical properties. *J. Alloys Compd.* 647, 392–396. <http://dx.doi.org/10.1016/j.jallcom.2015.06.076>.
- [4] Thakkar, K.N., Mhatre, S.S., Parikh, R.Y., 2010. Biological synthesis of metallic nanoparticles. *Nanomed. Nanotechnol. Biol. Med.* 6, 257–262. <http://dx.doi.org/10.1016/j.nano.2009.07.002>
- [5] Diallo, A., Beye, A.C., Doyle, T.B., Park, E., Maaza, M., 2015. Green synthesis of Co₃O₄ nanoparticles via *Aspalathus linearis*: physical properties. *Green Chem. Lett. Rev.* 8, 30–36. <http://dx.doi.org/10.1080/17518253.2015.1082646>.
- [6] Thema, F.T., Beukes, P., Gurib-Fakim, A., Maaza, M., 2015a. Green synthesis of Montepelite CdO nanoparticles by *Agathosma betulina* natural extract. *J. Alloys Compd.* 646, 1043–1048. <http://dx.doi.org/10.1016/j.jallcom.2015.05.279>.
- [7] Thema, F.T., Manikandan, E., Dhlamini, M.S., Maaza, M., 2015b. Green synthesis of ZnO nanoparticles via *Agathosma betulina* natural extract. *Mater. Lett.* 161, 124–127. <http://dx.doi.org/10.1016/j.matlet.2015.08.052>.
- [8] Thovhogi, N., Diallo, A., Gurib-Fakim, A., Maaza, M., 2015. Nanoparticles green synthesis by Hibiscus Sabdariffa flower extract: main physical properties. *J. Alloys Compd.* 647, 392–396. <http://dx.doi.org/10.1016/j.jallcom.2015.06.076>.
- [9] Sone, B.T., Manikandan, E., Gurib-Fakim, A., Maaza, M., 2015. Sm₂O₃ nanoparticles green synthesis via *Callistemon viminalis*’ extract. *J. Alloys Compd.* 650, 357–362. <http://dx.doi.org/10.1016/j.jallcom.2015.07.272>.
- [10] Konwarh, R., Karak, N., Sawian, C.E., Baruah, S., Mandal, M., 2011. Effect of sonication and aging on the templating attribute of starch for “green” silver nanoparticles and their interactions at biointerface. *Carbohydr. Polym.* 83, 1245–1252. <http://dx.doi.org/10.1016/j.carbpol.2010.09.031>.
- [11] Tran, H.V., Tran, L.D., Ba, C.T., Vu, H.D., Nguyen, T.N., Pham, D. G., Nguyen, P.X., 2010. Synthesis, characterization, antibacterial and antiproliferative activities of monodisperse chitosan-based silver nanoparticles. *Colloids Surf. A Physicochem. Eng. Asp.* 360, 32–40. <http://dx.doi.org/10.1016/j.colsurfa.2010.02.007>.
- [12] Quelemes, P., Araruna, F., de Faria, B., Kuckelhaus, S., da Silva, D., Mendonça, R., Eiras, C., Soares, M. dos S., Leite, J.R., 2013. Development and antibacterial activity of cashew gum-based silver nanoparticles. *Int. J. Mol. Sci.* 14, 4969–4981. <http://dx.doi.org/10.3390/ijms14034969>.
- [13] Venkatapurwar, V., Pokharkar, V., 2011. Green synthesis of silver nanoparticles using marine polysaccharide: study of in-vitro antibacterial activity. *Mater. Lett.* 65, 999–1002. <http://dx.doi.org/10.1016/j.matlet.2010.12.057>.
- [14] Xia, N., Cai, Y., Jiang, T., Yao, J., 2011. Green synthesis of silver nanoparticles by chemical reduction with hyaluronan. *Carbohydr. Polym.* 86, 956–961. <http://dx.doi.org/10.1016/j.carbpol.2011.05.053>.
- [15] Wijesekara, I., Pangestuti, R., Kim, S.-K., 2011. Biological activities and potential health benefits of sulfated polysaccharides derived from marine algae. *Carbohydr. Polym.* 84, 14–21. <http://dx.doi.org/10.1016/j.carbpol.2010.10.062>.
- [16] Carneiro, J.G., Rodrigues, J.A.G., Teles, F.B., Cavalcante, A.B.D., Benevides, N.M.B., 2014. Analysis of some chemical nutrients in four Brazilian tropical seaweeds. *Acta Sci. Biol. Sci.* 36, 137–145. <http://dx.doi.org/10.4025/actasciobiolsci.v36i2.19328>.
- [17] Coura, C.O., de Araújo, I.W.F., Vanderlei, E.S.O., Rodrigues, J.A.G., Quindere, A.L.G., Fontes, B.P., de Queiroz, I.N.L., de Menezes, D. B., Bezerra, M.M., e Silva, A.A.R., Chaves, H.V., Jorge, R.J.B., Evangelista, J.S.A.M., Benevides, N.M.B., 2012. Antinociceptive and anti-inflammatory activities of sulphated polysaccharides from the red seaweed *Gracilaria cornea*. *Basic Clin. Pharmacol. Toxicol.* 110, 335–341. <http://dx.doi.org/10.1111/j.1742-7843.2011.00811.x>.
- [18] Maciel, J., Chaves, L., Souza, B., Teixeira, D., Freitas, A., Feitosa, J., Depaula, R., 2008. Structural characterization of cold extracted fraction of soluble sulfated polysaccharide from red seaweed *Gracilaria birdiae*. *Carbohydr. Polym.* 71, 559–565. <http://dx.doi.org/10.1016/j.carbpol.2007.06.026>.
- [19] Souza, B.W.S., Cerqueira, M.A., Bourbon, A.I., Pinheiro, A.C., Martins, J.T., Teixeira, J.A., Coimbra, M.A., Vicente, A.A., 2012. Chemical characterization and antioxidant activity of sulfated polysaccharide from the red seaweed *Gracilaria birdiae*. *Food Hydrocoll.* 27, 287–292. <http://dx.doi.org/10.1016/j.foodhyd.2011.10.005>.
- [20] Chattopadhyay, K., Ghosh, T., Pujol, C.A., Carlucci, M.J., Damonte, E.B., Ray, B., 2008. Polysaccharides from *Gracilaria corticata*: sulfation, chemical characterization and anti-HSV activities. *Int. J. Biol. Macromol.* 43, 346–351. <http://dx.doi.org/10.1016/j.ijbiomac.2008.07.009>.
- [21] Pal Sovan Lal, Utpal Jana PK, Manna GP, Mohanta Manavalan R (2011) Nanoparticle: an overview of preparation and characterization. *J Appl Pharma Sci* 1(6):228–234
- [22] Auffan M, Rose J, Bottero JY, Lowry GV, Jolivet JP, Wiesner MR (2009) Towards a definition of inorganic nanoparticles from an environmental, health and safety perspective. *Nat Nanotechnol* 4:634–641

- [23] Supraja N, Prasad TNVKV, Giridhar Krishna T, David E (2015) Synthesis, Characterization and Evaluation of the antimicrobial efficacy of *Boswellia ovalifoliolata* stem bark extract mediated zinc oxide nanoparticles. Applied nanoscience DOI 10.1007/s13204-015-0472-0
- [24] He Y, Wan TJM, Tokunaga T (2008) Kinetic stability of hematite nanoparticles of the effect of particle sizes. J. Nanoparticle Res 10: 321–332
- [25] Turner and Timothy (2012) Development of the Polio Vaccine: A Historical Perspective of Tuskegee University's Role in Mass Production and Distribution of HeLa Cells. *Journal of Health Care for the Poor and Underserved*. 23 (4a): 5–10.doi:10.1353/hpu.2012.0151



Fig 1: *Gracilaria corticata*

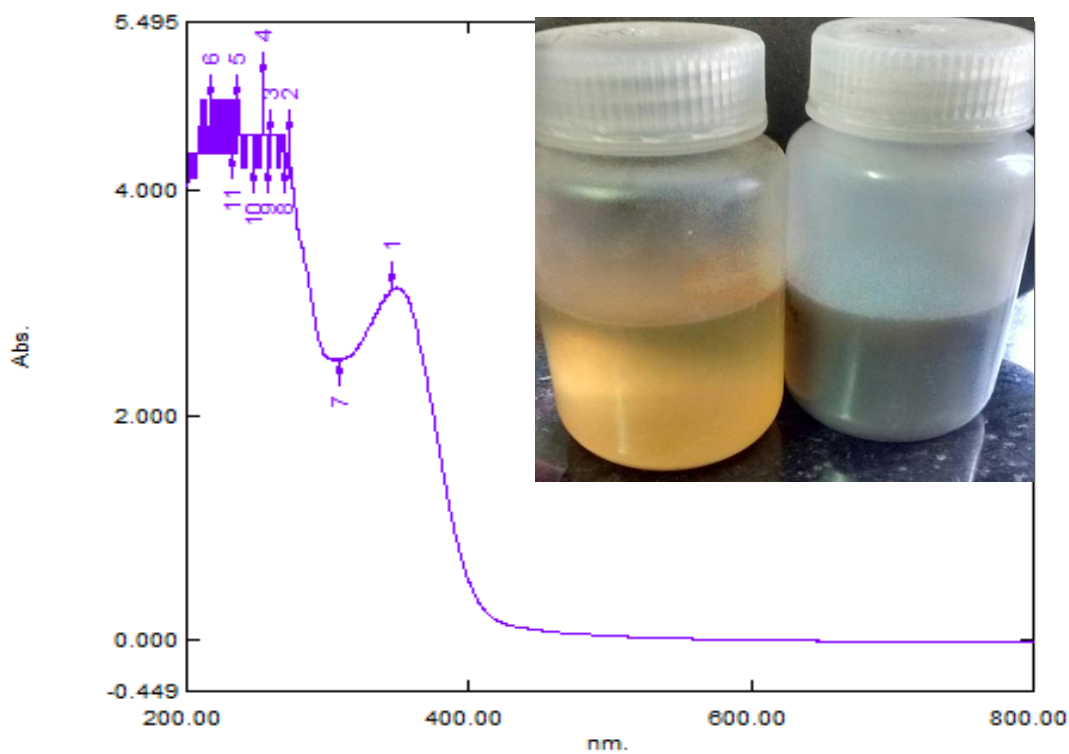


Fig 2: UV-visible spectroscopy showing *Gracilaria corticata* mediated synthesized silver nanoparticles

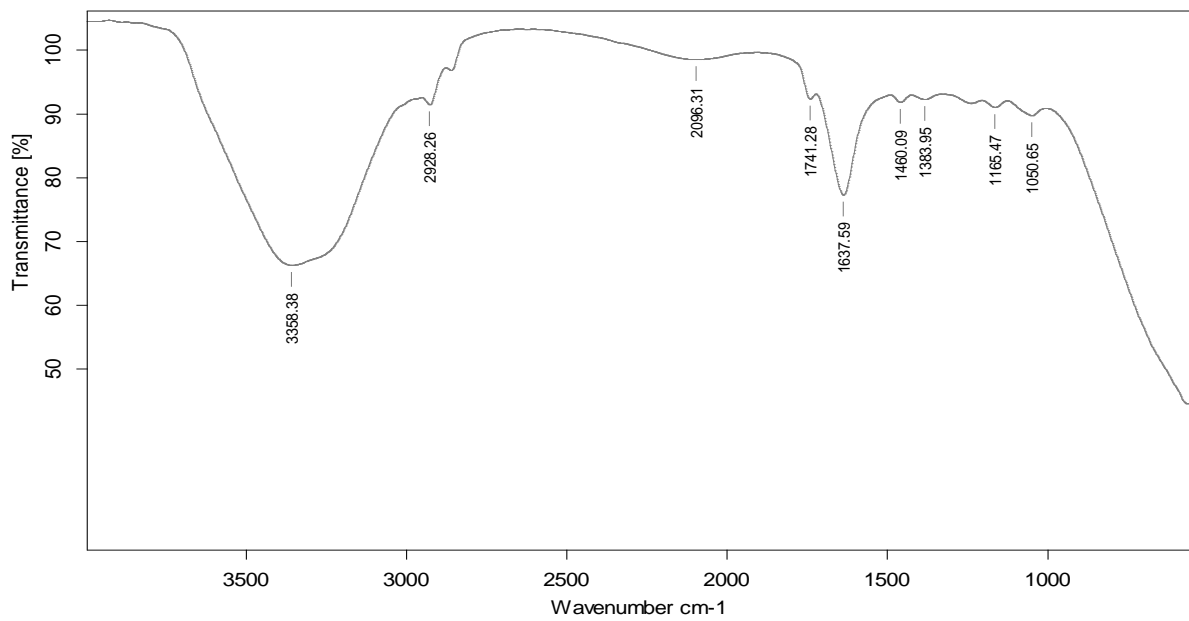


Fig 3: FT-IR spectroscopy showing *Gracilaria corticata* mediated synthesized silver nanoparticles

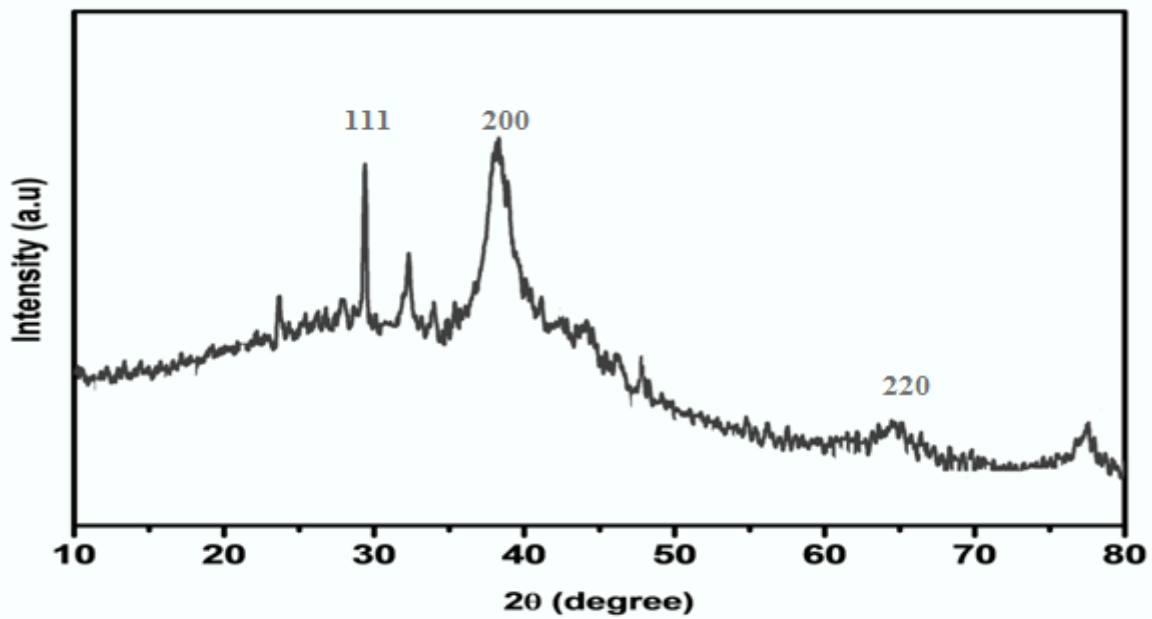


Fig 4: XRD analysis showing *Gracilaria corticata* mediated synthesized silver nanoparticles

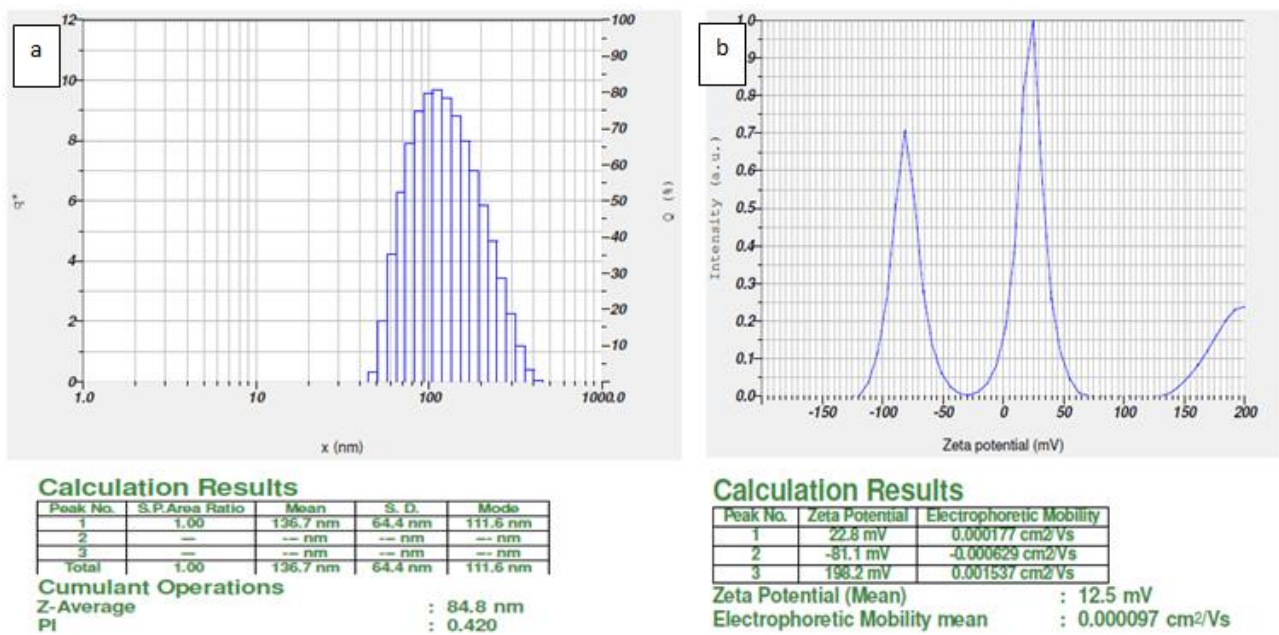


Fig 5: DLS analysis showing a) Particle size b) Zeta potential *Gracilaria corticata* mediated synthesized silver nanoparticles

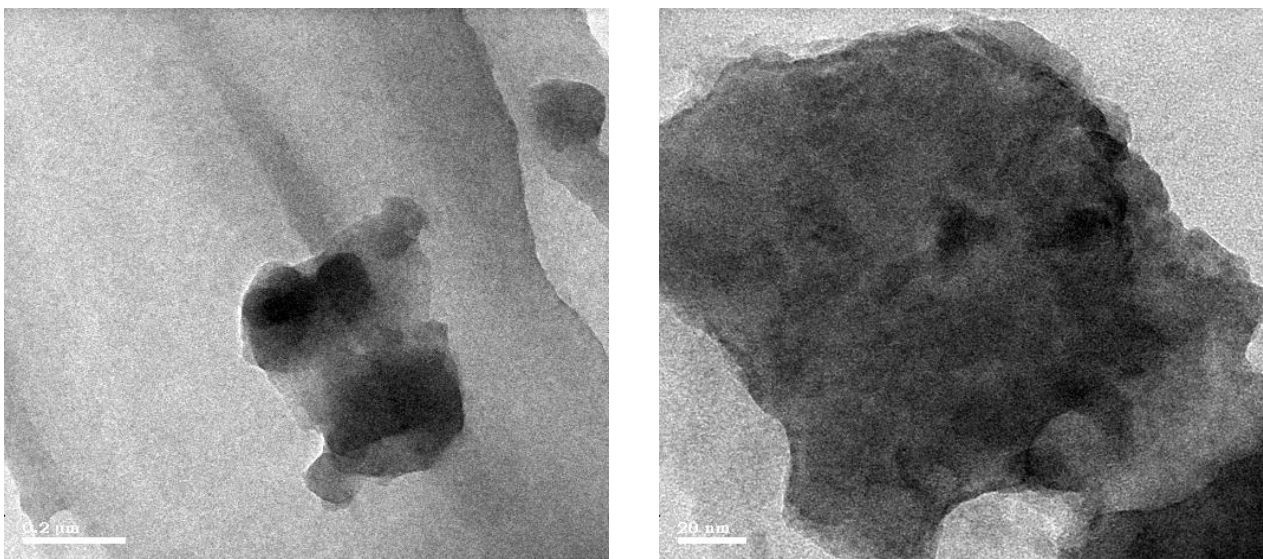
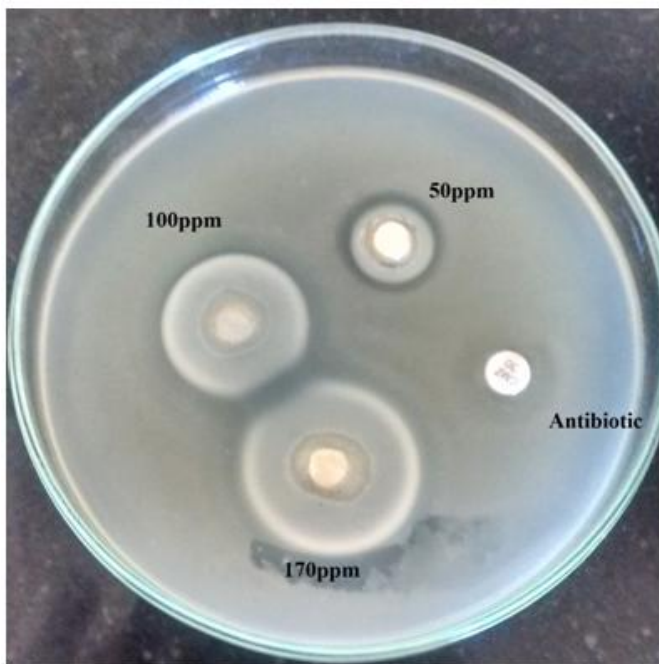
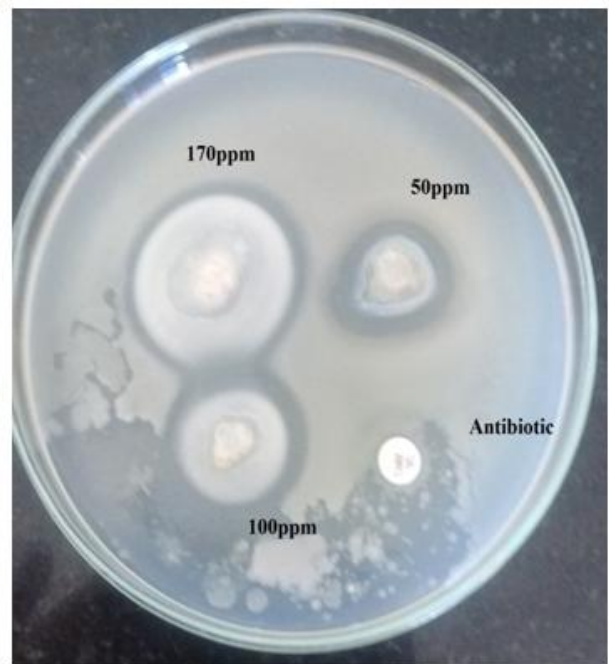


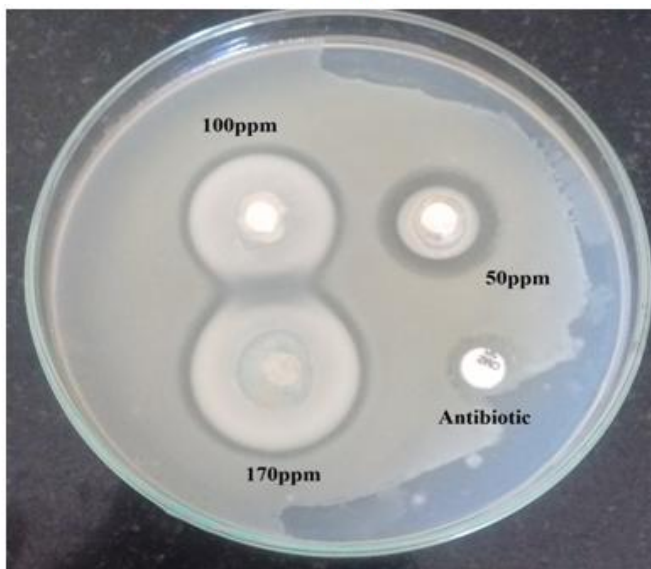
Fig 6: Showing TEM images of *Gracilaria corticata* mediated synthesis of silver nanoparticles



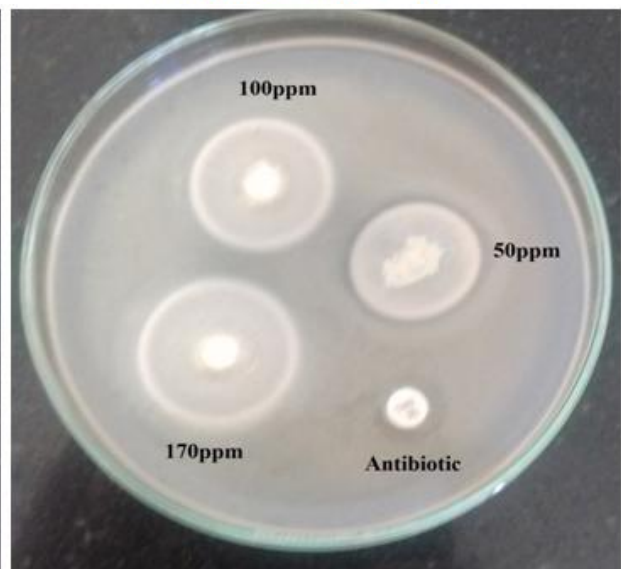
E. coli



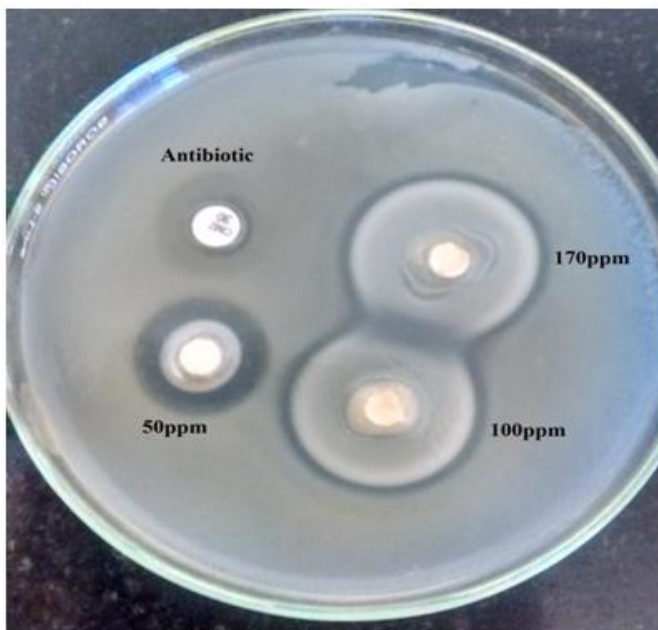
Pseudomonas Fluorescence



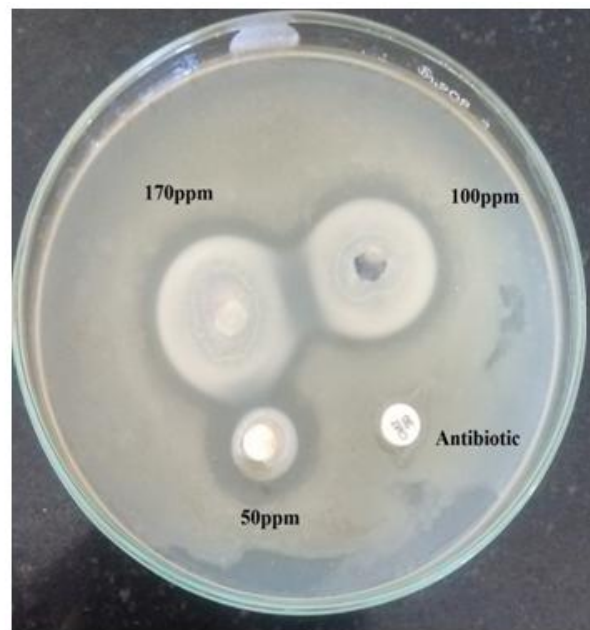
Staphylococcus aureus



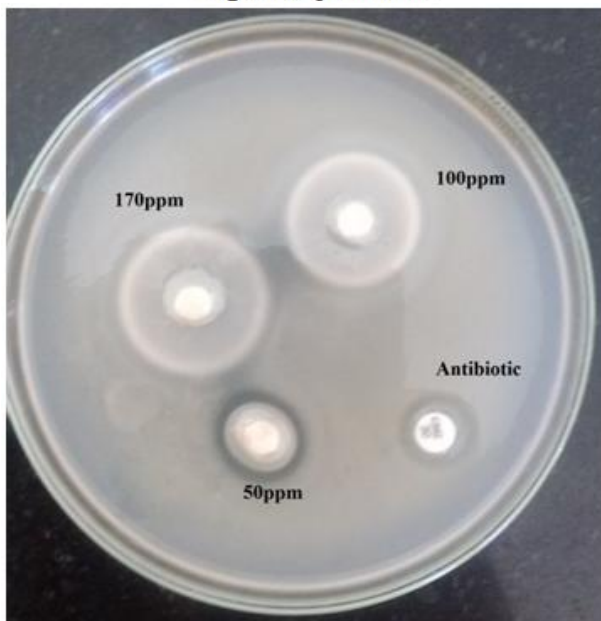
Sphingobacterium thalpophilum



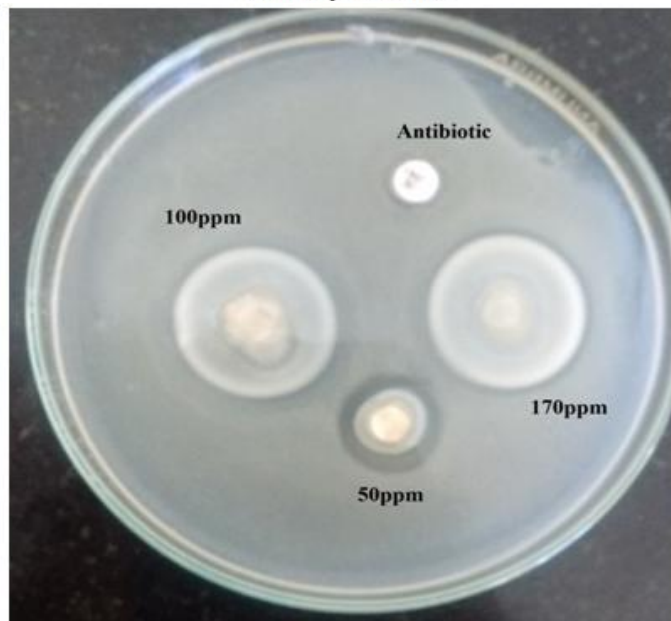
Legionella pneumonia



Actinomyces israelii



Enterobacter cloacae



Helicobacter pylori

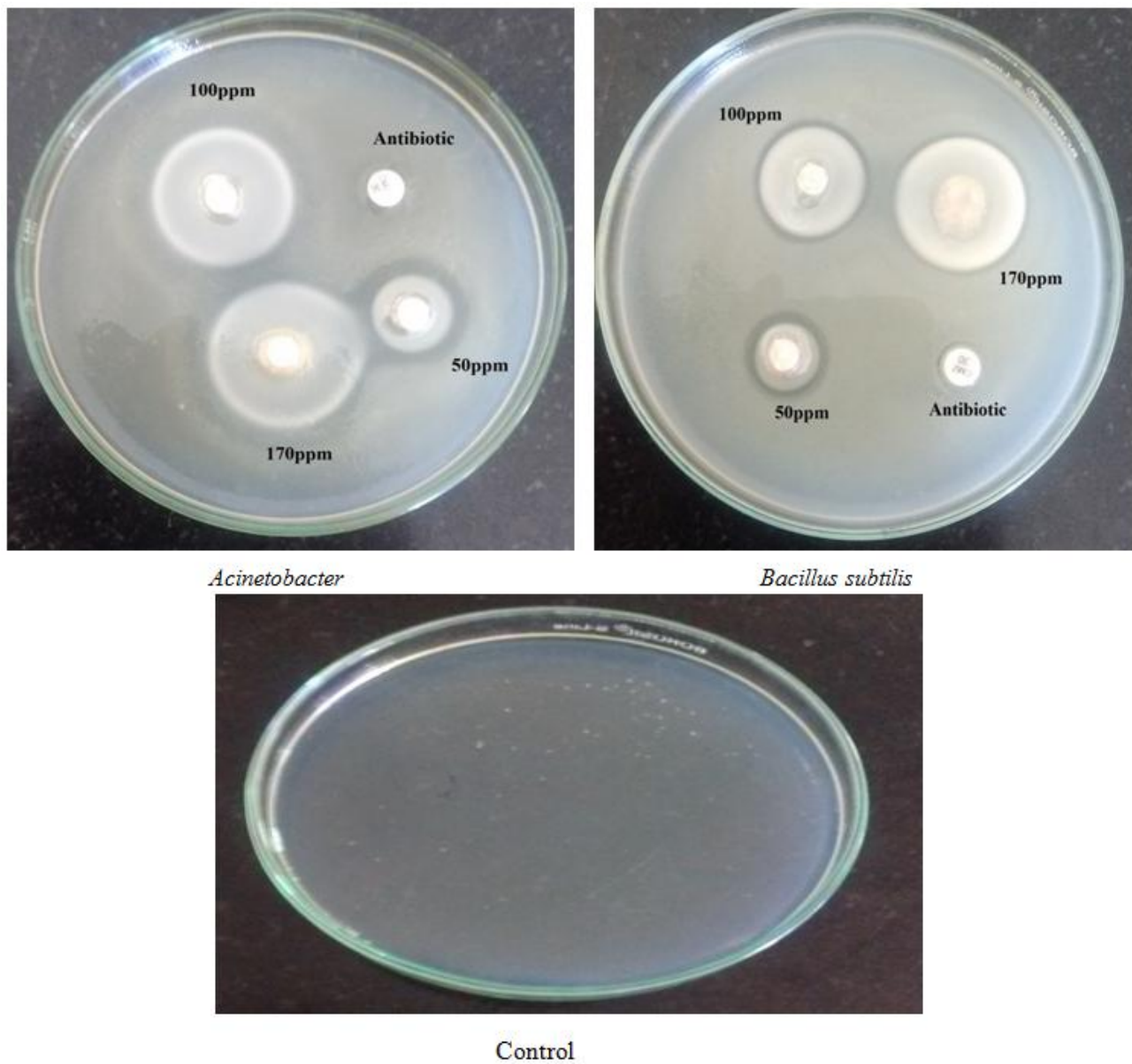
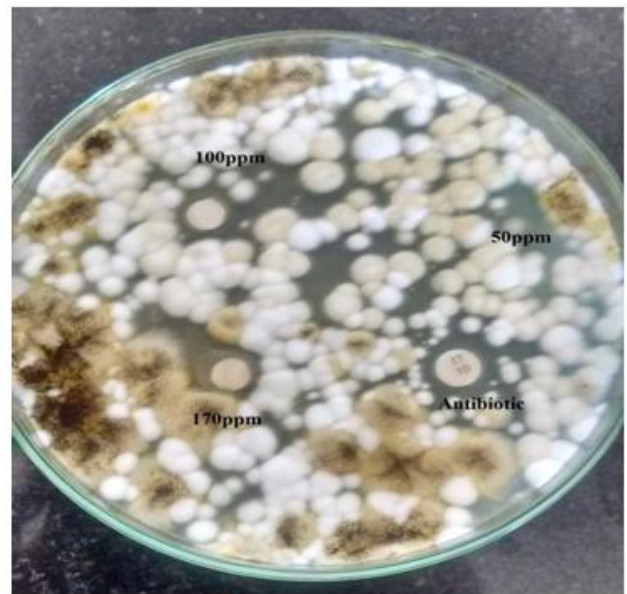


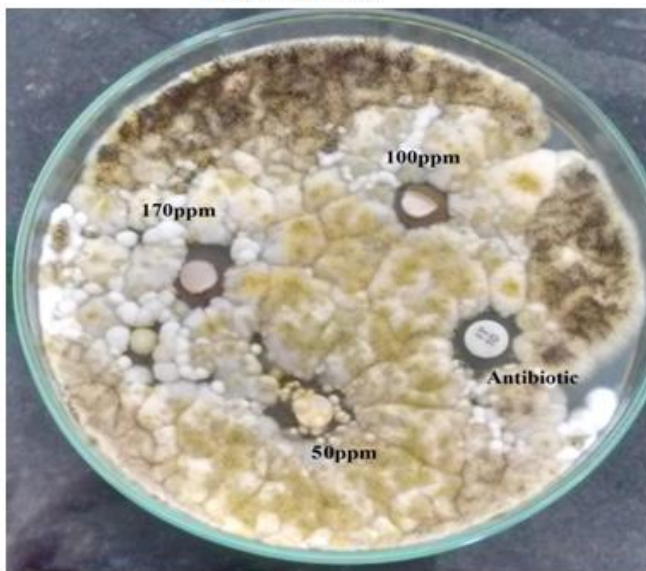
Fig 7a: showing antibacterial activity of *Gracilaria corticata* mediated synthesis of silver nanoparticles



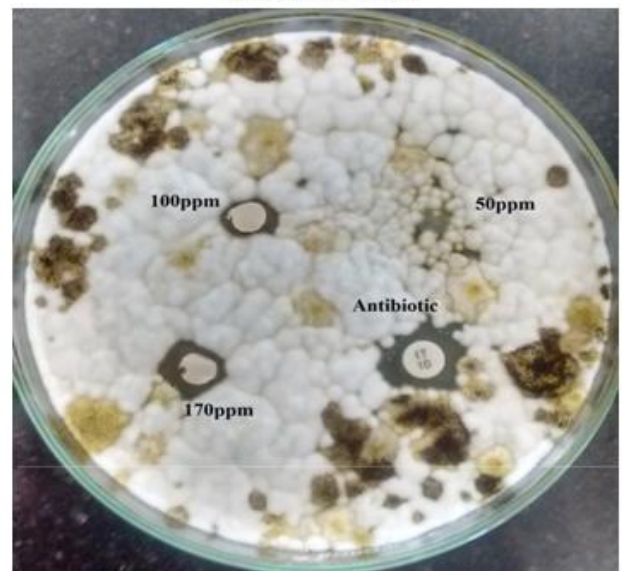
Aspergillus niger



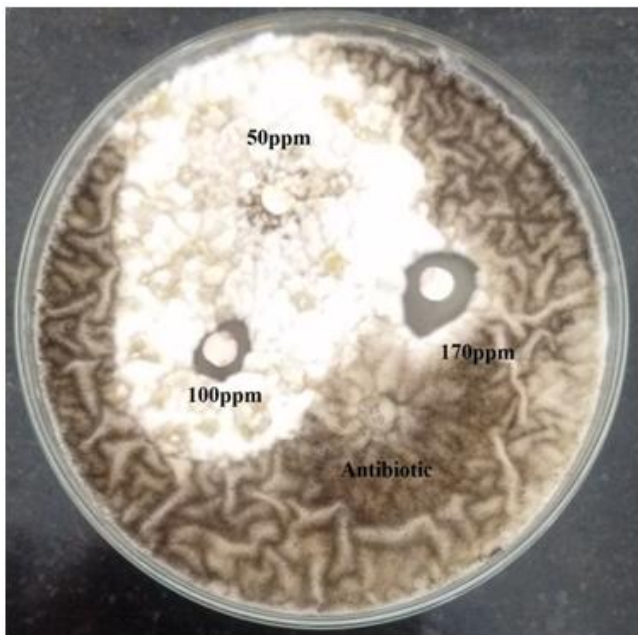
Aspergillus flavus



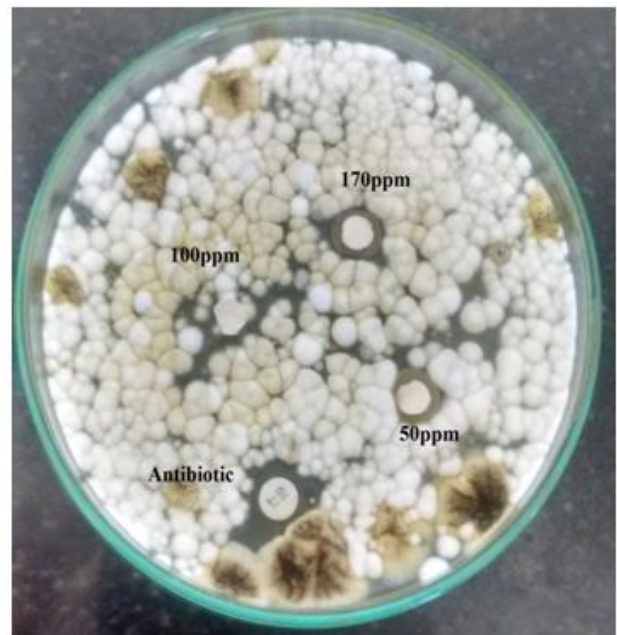
Schelorosium rolfsii



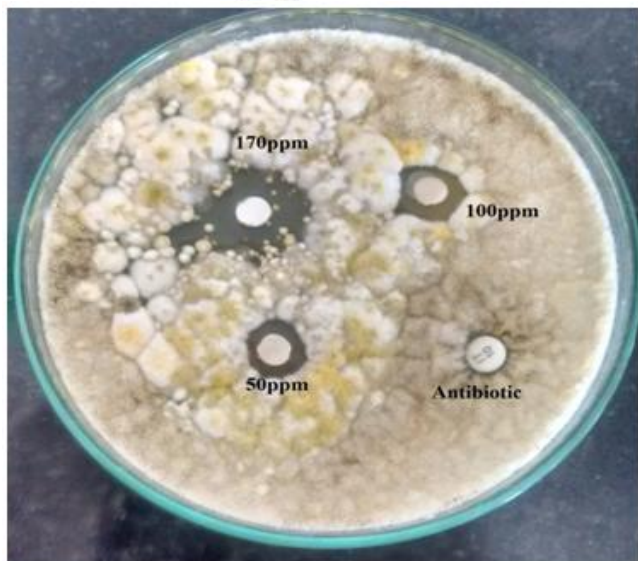
Rhizopus oligosporus



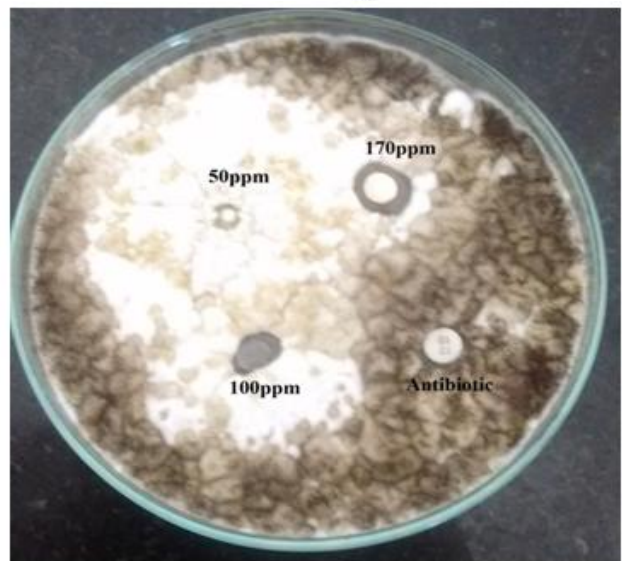
Aspergillus acidus



Athelia rolfsii



Aspergillus fumigatus



Rhizopus oryzae

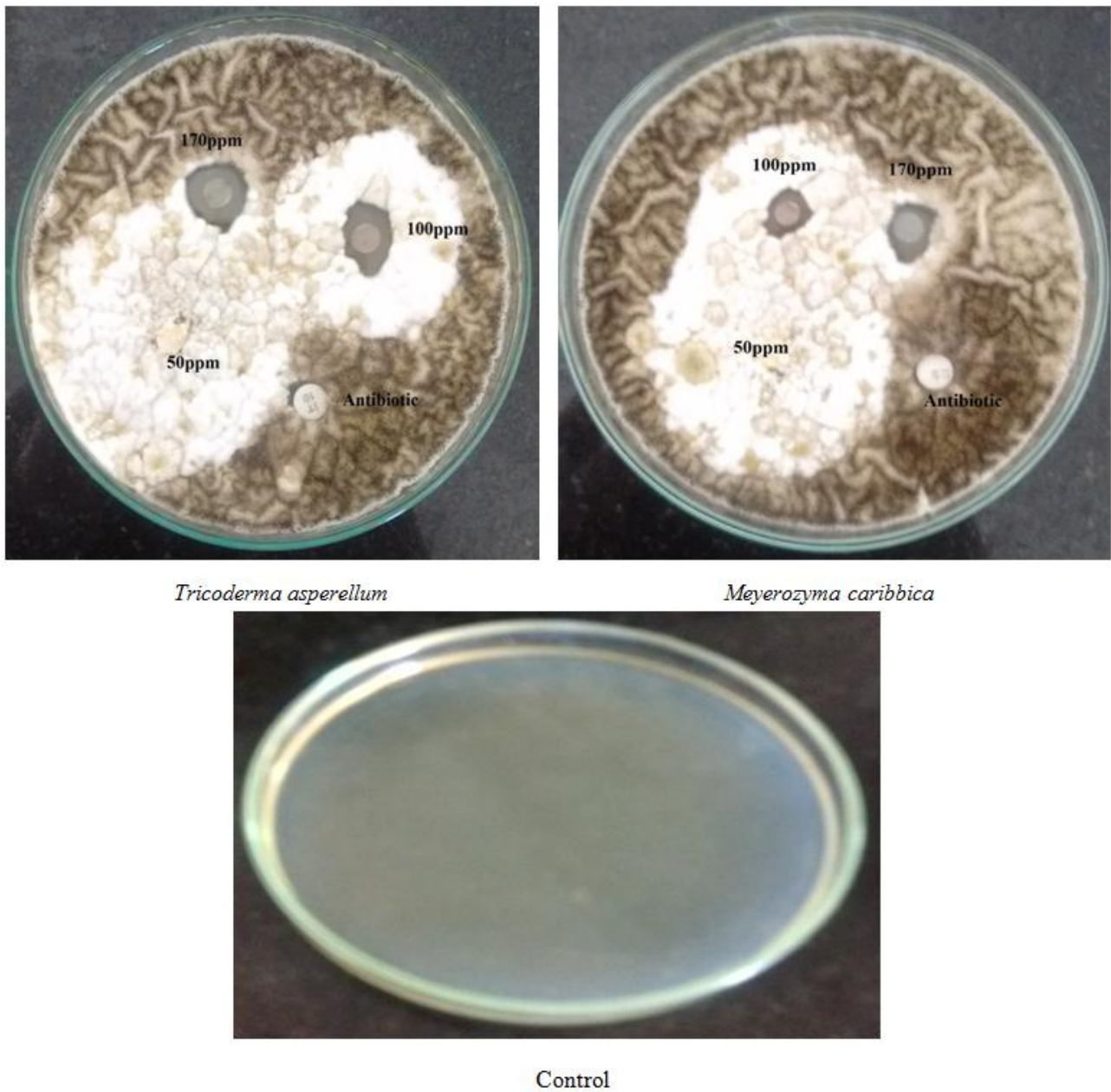
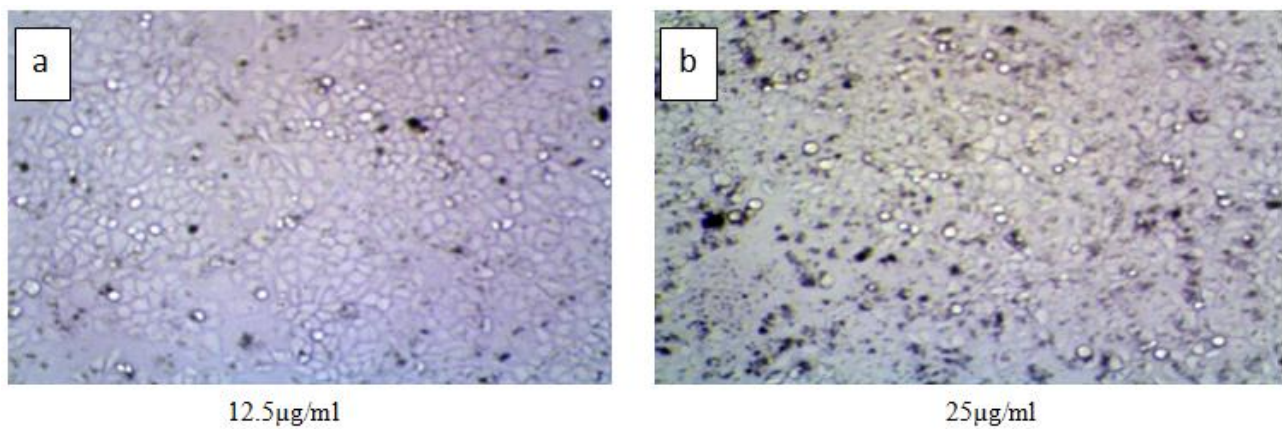


Fig 7b: Showing antifungal activity of *Gracilaria corticata* mediated synthesis of silver nanoparticles



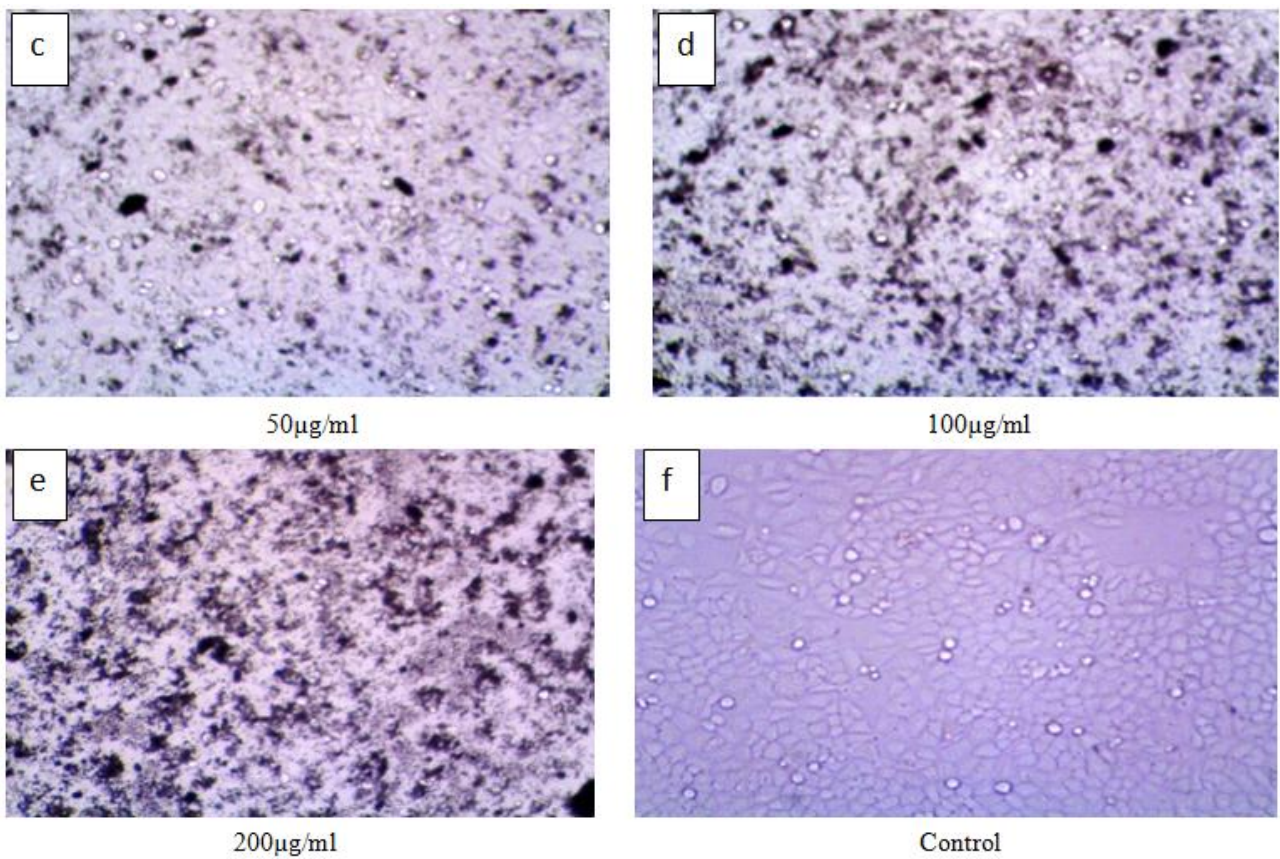


Fig 8: Human Cervical cancer cell line (HeLa) treated with 12.5-200 µg/ml of synthesized AgNPs using *Gracilaria corticata* aqueous extract

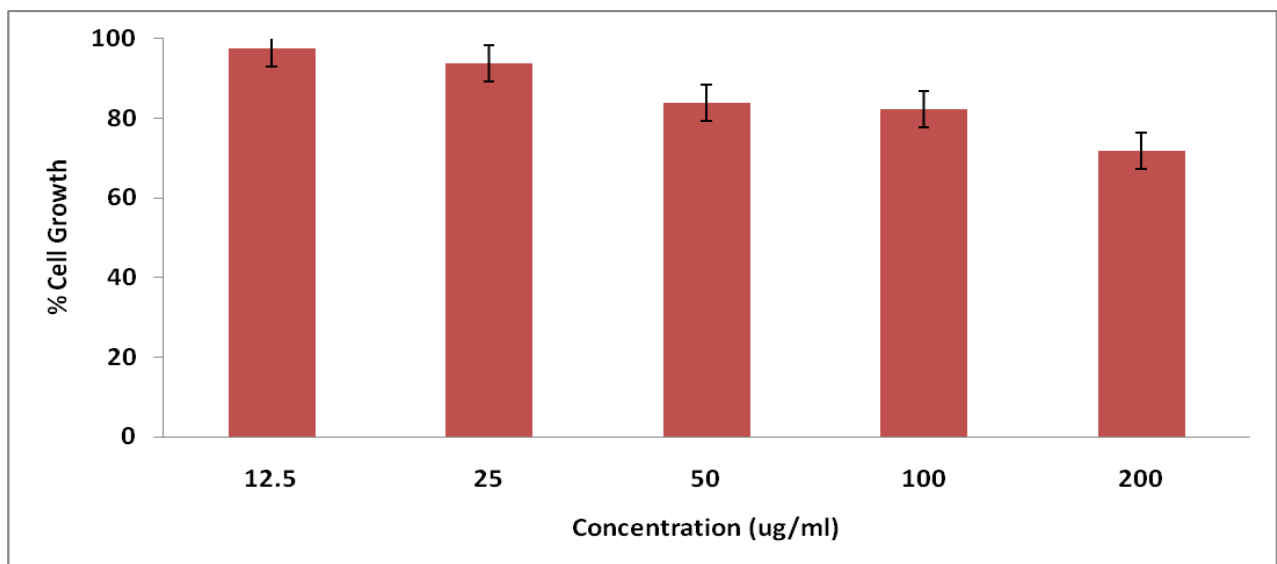


Fig 9: Cytotoxic activity of *Gracilaria corticata* AgNPs against Human Cervical cancer cell line (HeLa)

Table I: In-vitro antibacterial studies using *Gracilaria corticata* mediated synthesis of silver nanoparticles

S.No.	Name of Bacteria	170±1.4ppm	100±1.1ppm	50±0.8ppm	Penicilin-G (30mcg)
1	<i>E. coli</i>	2.6±0.12	2.3±0.10	2.2±0.08	1.0
2	<i>Pseudomonas Fluorescence</i>	2.5±0.11	2.2±0.09	1.8±0.06	1.0
3	<i>Staphylococcus aureus</i>	2.2±0.09	2.1±0.08	2.0±0.09	1.1
4	<i>Sphingobacterium thalpophilum</i>	2.3±0.10	2.2±0.09	1.9±0.07	1.0
5	<i>Legionella pneumonia</i>	2.6±0.11	2.5±0.10	1.9±0.07	1.0
6	<i>Actinomyces israelii</i>	2.1±0.09	2.0±0.08	1.8±0.06	0.8
7	<i>Enterobacter cloacae</i>	3.0±0.14	3.0±0.13	2.8±0.12	1.0
8	<i>Helicobacter pylori</i>	2.2±0.09	2.1±0.09	1.8±0.06	1.0
9	<i>Acinetobacter</i>	2.9±0.12	2.6±0.11	2.0±0.09	1.0
10	<i>Bacillus subtilis</i>	2.6±0.11	2.2±0.09	2.1±0.09	1.1

Each value is the ±SE of three measurements

Table II: In-vitro antifungal studies using *Gracilaria corticata* mediated synthesis of silver nanoparticles

S.No.	Name of Fungus	170±ppm	100±ppm	50±ppm	Itraconazole (30mcg)
1	<i>Aspergillus niger</i>	2.1±0.12	1.9±0.10	1.5±0.06	0.8
2	<i>Aspergillus flavus</i>	2.3±0.13	1.6±0.08	1.1±0.05	0.6
3	<i>Schelorosium rolfisii</i>	2.5±0.15	1.7±0.09	1.2±0.06	0.6
4	<i>Rhizopus oligosporus</i>	2.8±0.17	2.0±0.10	1.0±0.05	0.9
5	<i>Aspergillus acidus</i>	1.6±0.09	1.2±0.06	0.8±0.04	0.6
6	<i>Athelia rolfisii</i>	2.6±0.14	1.8±0.09	0.5±0.03	0.4
7	<i>Aspergillus fumigates</i>	1.5±0.08	1.1±0.07	0.6±0.05	0.4
8	<i>Rhizopus oryzae</i>	2.1±0.11	1.6±0.08	1.1±0.05	0.8
9	<i>Tricoderma asperellum</i>	2.0±0.10	1.9±0.09	0.9±0.06	0.5
10	<i>Meyerozyma caribbica</i>	2.1±0.11	1.8±0.08	1.0±0.06	0.9

Each value is the ±SE of three measurements

Table III: Cytotoxic activity of *Gracilaria corticata* AgNPs against Human Cervical cancer cell line (HeLa)

Conc ($\mu\text{g/ml}$)	% Cell viability
12.5	97.6109
25	93.8566
50	83.7884
100	82.1956
200	71.8998